

The role of acceptance angle in measurements with ion energy analyzers: Study by numerical simulations

W. J. Miloch, N. Gulbrandsen, L. N. Mishra, and Å. Fredriksen

Citation: *Appl. Phys. Lett.* **97**, 261501 (2010); doi: 10.1063/1.3531757

View online: <http://dx.doi.org/10.1063/1.3531757>

View Table of Contents: <http://aip.scitation.org/toc/apl/97/26>

Published by the [American Institute of Physics](#)

Fearful for the future of science?

Sign up for **FREE** FYI emails.
AIP | American Institute of Physics

The role of acceptance angle in measurements with ion energy analyzers: Study by numerical simulations

W. J. Miloch,^{a)} N. Gulbrandsen, L. N. Mishra, and Å. Fredriksen

Department of Physics and Technology, University of Tromsø, 9037 Tromsø, Norway

(Received 25 September 2010; accepted 6 December 2010; published online 29 December 2010)

The importance of an acceptance angle in the plasma diagnostics with ion energy analyzers is investigated by means of numerical simulations. It is shown that wide acceptance angles result in low energy tails in measured ion distribution functions (IDF_x). For flowing plasmas or plasmas with beams, the orientation of the analyzer's orifice gives different results due to bending of ion trajectories in the vicinity of the analyzer. It is demonstrated that the maximum in the IDF_x is at energies lower than the plasma potential. Simulations are done with DIP3D, a three-dimensional particle-in-cell code. © 2010 American Institute of Physics. [doi:10.1063/1.3531757]

Ion energy analyzers have become a standard diagnostic tool in processing plasmas, laboratory plasma experiments, and on satellite and rocket payloads.^{1–6} They allow for reliable measurements of ion velocity distributions, detection of beams, and determination of the plasma potential.^{1,2} The housing of an analyzer is often grounded, which can result in a large bias with respect to the plasma potential, and strong acceleration of plasma particles through the sheath.⁷

An example is the retarding field energy analyzer (RFEA), in which a series of biased grids is used to determine the energy of a particle entering the orifice.^{2,8} RFEAs are often used for diagnostics of ions because the derivative of the ion current to the collector with respect to the discriminator bias is proportional to the ion velocity distribution.

For the analysis of experimental data, a simplified, one-dimensional theory is usually applied,¹ and it is assumed that the result corresponds to the particle energy. This could be argued for directional energy analyzers with capillary plates or focusing devices,^{9–11} or effectively one-dimensional systems with fast beams or strong magnetic fields.⁸ However, usually, energy analyzers measure the particle momentum in the direction normal to the aperture,^{12,13} and the resulting current does not need to reflect the total energy of the particles. In this letter we will use a term *one-dimensional ion distribution function* (IDF_x) when referring to the derivative of the ion current to the analyzer.

It has been shown theoretically that the acceptance angle can modify the ion current, and therefore lead to changes in the IDF_x .^{12,13} Thus, this problem is crucial for data analysis. The energy analyzers can have different, but in most cases fixed geometry of orifices.^{6,9,11} The design of an analyzer with varied acceptance angle is challenging, and thus it is also difficult to study experimentally the role of this angle in the measurements with ion energy analyzers.

We address the problem of the acceptance angle in the measurements with ion energy analyzers with particle-in-cell (PIC) numerical simulations. We employ the DIP3D code, which has been designed for simulations of objects in complex plasma environments.^{14–16} For the present study, the code has been upgraded to account also for an external uni-

form magnetic field,¹⁷ and collisions.¹⁸ We simulate argon plasma with parameters close to the conditions in the helicon plasma device *Njord*.¹⁹ The plasma density is $n=10^{14} \text{ m}^{-3}$, and the neutral gas density $n_n=2 \times 10^{19} \text{ m}^{-3}$. The electron and ion temperatures are $T_e=7 \text{ eV}$ and $T_i=0.7 \text{ eV}$, respectively, resulting in the Debye length $\lambda_D=0.6 \text{ mm}$. The plasma is weakly magnetized with $B=0.1 \text{ mT}$. For these plasma parameters, we consider plasma that is stationary or flowing with a subsonic velocity along the x axis.

A spherical analyzer of diameter $d \approx 1.1 \text{ cm}$ is placed in the center of the simulation box of length $L=10 \text{ cm}$ in each direction. The orifice of radius $a/d \approx 0.1$ and varied acceptance angle θ is directed either upstream or downstream. The scheme of numerical environment is shown in Fig. 1. Note that this geometry is similar to some electrostatic probes.^{20,21} The surface of the analyzer is equipotential, and its potential is set $\Phi=-45 \text{ V}$ with respect to the plasma potential, in order to simulate the experimental condition of a grounded analyzer in an electropositive plasma.

IDF_x 's obtained for stationary plasma and different acceptance angles θ are shown in Fig. 2(a). We assume that there are no focusing effects inside the analyzer, and all plasma particles entering the orifice contribute to the current. The corresponding ion energy distribution function, obtained from the total momentum of the particles entering the orifice, is shown in Fig. 2(b). The shape of the IDF_x at lower energies, as well as the strength of the signal, changes with θ . Wide acceptance angles give stronger signals at the expense of developing a low energy tail in the IDF_x , while for very small θ , the shape of the IDF_x becomes similar to the ion energy distribution function. The low energy tails are due to ions entering the aperture at large inclination angles, so that a significant part of their momentum is in the tangential com-

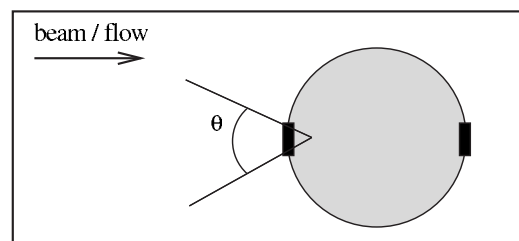


FIG. 1. The scheme of numerical environment.

^{a)}Electronic mail: wojciech.j.miloch@uit.no.

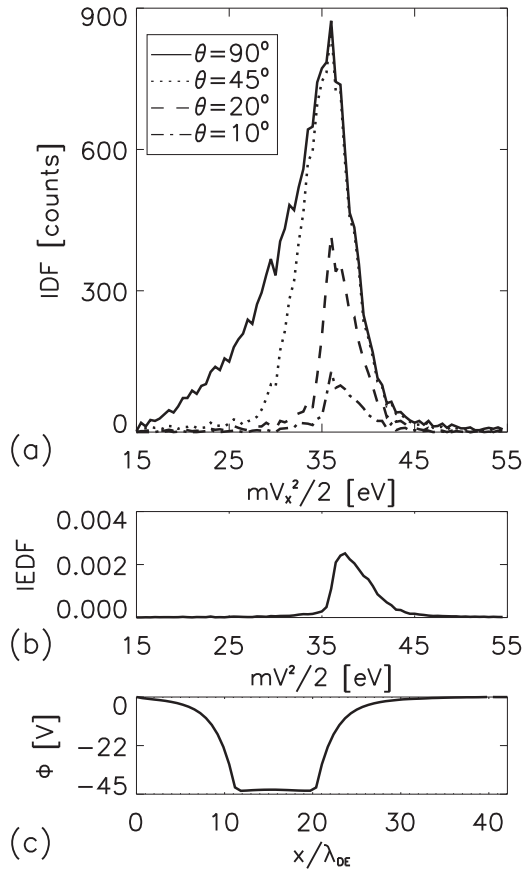


FIG. 2. Simulation results for stationary plasma: (a) IDF_x for different acceptance angles θ (the results for $\theta=180^\circ$ are similar to $\theta=90^\circ$; thus they are not shown here), (b) ion energy distribution function (normalized), and (c) cut through the averaged potential along the x axis at $y=z=L/2$.

ponent of the velocity. With decreasing θ , the low energy tail in the IDF_x diminishes, while the position of peak, and the shape of the IDF_x for higher discriminator bias do not change significantly. This confirms that the low energy tail is an artifact due to the acceptance angle, which should be accounted for in the analysis of experimental data.

The effect of θ is more pronounced for flowing plasmas. The wake formation and bending of ion trajectories by electric fields in the sheath, often referred to as ion focusing,^{20–22} can lead to a large tangential velocity component for particles reaching the rear of the analyzer. Thus, a wide acceptance angle of the analyzer facing downstream can result in an enhanced IDF_x at low energies; see Fig. 3. On the upstream side, the peak of the IDF_x is shifted toward higher energies, and the effect of θ is less visible.

The influence of an acceptance angle on the shape of the IDF_x at lower energies affects the measurements of the plasma potential with ion energy analyzers. The maximum of the IDF_x should according to the one-dimensional theory correspond to the plasma potential, and then be the onset of the exponential decrease in the ion saturation current.^{1,23} The plasma potential is often chosen at the maximum of the Gaussian fit to the IDF_x .^{24,25} Our simulations show that the peak in the IDF_x is placed toward lower energies with respect to the plasma potential. The averaged potential profile cut through the simulation box for stationary plasma is shown in Fig. 2(c). From comparing it with Fig. 2(a), we see that the peak in the IDF_x is at lower energies ($mv_x^2/2 \approx 37$ eV) than the total potential drop in the sheath and

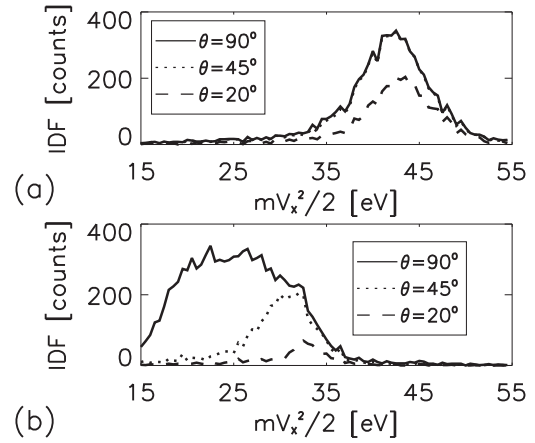


FIG. 3. IDF_x from the simulations of plasma with a subsonic flow (0.75 Mach) for different θ , and the orifice of the analyzer oriented (a) upstream and (b) downstream. In (a) IDF_x for $\theta=90^\circ$ is almost the same as for $\theta=45^\circ$.

presheath ($\Delta\Phi=45$ V). This shift is comparable to the electron energy, and could be associated with the potential drop in the presheath. We observe corresponding shifts also in simulations with other plasma parameters, as well as for collisionless plasmas. Thus the peak of the IDF_x can be associated with the plasma potential in close vicinity to the analyzer. We note that some have used the end of the distribution as the plasma potential at the source,²³ indicating that these energies correspond to ions accelerated by the total potential drop in the system. In our simulations the plasma potential corresponds to the undisturbed Maxwellian plasma in the reservoirs adherent to the simulation box.

The position of a maximum in the IDF_x (or an onset of the exponential decrease in the ion saturation current) is more robust and easily measured than the point referring to the plasma potential. Thus, it is a better candidate for determining the plasma potential, although one should acknowledge a systematic error toward lower potential values.

An ion beam provides yet another intricacy to the system. To demonstrate the importance of the opening angle for beam measurements, we simulate a typical plasma for beam conditions in the Njord device:¹⁹ $n=2.5 \times 10^{16}$ m⁻³, $B=0.02$ T, $T_e=4$ eV, and $T_i=0.4$ eV. A supersonic beam of $n=8 \times 10^{15}$ m⁻³ is introduced in the central part of the simulation box. Due to computational limitations, only a very small region can be simulated, $L=4 \times 10^{-3}$ m in each direction, and the radius of the analyzer is 25 times smaller than in the laboratory experiment. However, it is still one order of magnitude larger than the Debye length. To ensure correct scaling (i.e., the analyzer is larger than the Debye length and the electron Larmor radius, and smaller than the ion Larmor radius and ion mean free path), we apply a stronger magnetic field ($B=0.6$ T). The potential of the analyzer is again set at $\Phi=-45$ V with respect to the plasma potential.

A supersonic beam leads to different signals from the front and rear of the analyzer, with the beam being detected on the front side. For large θ , a significant low energy component is present at the rear side, due to bending of beam particle trajectories. For $\theta=90^\circ$, we observe good qualitative agreement between the results from simulation and laboratory experiment; see Fig. 4. The measurements in the laboratory were done with RFEAs with $\theta \approx 80^\circ$.²⁶ We note that the present understanding of analyzers and probes in magne-

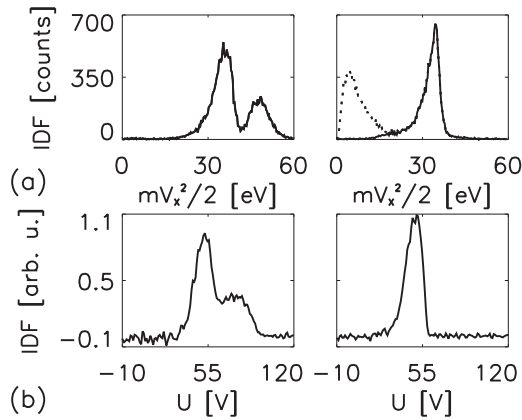


FIG. 4. (a) IDF_x from simulations for stationary plasma with supersonic beam (2.0 Mach), for the analyzer's orifice facing upstream (left) and downstream (right). The solid line is for $\theta=90^\circ$, while the dotted line is for $\theta=180^\circ$. (b) IDF_x from laboratory measurements in the Njord device for plasma with a beam (upstream—left and downstream—right; U refers to the RFEA discriminator bias).

tized plasmas is still limited. In our simulations a weak magnetic field was introduced only to reconstruct the experimental conditions, with ions being effectively unmagnetized. The object-plasma interactions in a strong magnetic field have recently been studied in other simulations.²⁷

With PIC simulations we studied the role of the acceptance angle on the ion distribution function obtained from measurements with ion energy analyzers. It has been demonstrated that the acceptance angle leads to an enhanced signal at lower energies, and that the position of the maximum in the ion distribution function, which is often used for determination of the plasma potential, can carry a systematic shift toward lower potential values.

This work was supported by the Norwegian Research Council, NFR Grant No. 177570.

- ¹M. Sugawara and B. R. Stansfield, *Plasma Etching: Fundamentals and Applications* (Oxford University Press, Oxford, 1998).
- ²I. H. Hutchinson, *Principles of Plasma Diagnostics* (Cambridge University Press, Cambridge, 2002).
- ³C. Charles, *Plasma Sources Sci. Technol.* **16**, R1 (2007).
- ⁴R. A. Pitts, R. Chavan, S. K. Erents, G. Kavaney, G. F. Matthews, G. Neil, J. E. Vince, I. Duran, and JET-EFTA Workshop Contributors, *Rev. Sci. Instrum.* **74**, 4644 (2003).
- ⁵R. L. Davidson, G. D. Earle, J. H. Klenzing, and R. A. Heelis, *Phys. Plasmas* **17**, 082901 (2010).
- ⁶M. J. Sablik, D. Golimowski, J. R. Sharber, and J. D. Winningham, *Rev. Sci. Instrum.* **59**, 146 (1988).
- ⁷J. E. Allen, *Plasma Sources Sci. Technol.* **18**, 014004 (2009).
- ⁸G. F. Matthews, *Plasma Phys. Controlled Fusion* **36**, 1595 (1994).
- ⁹R. L. Stenzel, R. Williams, R. Agüero, K. Kitazaki, A. Ling, T. McDonald, and J. Spitzer, *Rev. Sci. Instrum.* **53**, 1027 (1982).
- ¹⁰V. Kanarov, D. Siegfried, P. Sferlazzo, A. Hayes, and R. Yevtukhov, *Rev. Sci. Instrum.* **79**, 093304 (2008).
- ¹¹A. W. Molvik, *Rev. Sci. Instrum.* **52**, 704 (1981).
- ¹²J. A. Simpson, *Rev. Sci. Instrum.* **32**, 1283 (1961).
- ¹³J. R. Roth and M. Clark, *Plasma Phys.* **11**, 131 (1969).
- ¹⁴W. J. Miloch, *Plasma Phys. Controlled Fusion* **52**, 124004 (2010).
- ¹⁵W. J. Miloch, M. Kroll, and D. Block, *Phys. Plasmas* **17**, 103703 (2010).
- ¹⁶J. Olson, W. J. Miloch, S. Ratynskaya, and V. Yaroshenko, *Phys. Plasmas* **17**, 102904 (2010).
- ¹⁷C. K. Birdsall and A. B. Langdon, *Plasma Physics via Computer Simulation* (Adam Hilger, Bristol, 1991).
- ¹⁸V. Vahedi and M. Surendra, *Comput. Phys. Commun.* **87**, 179 (1995).
- ¹⁹Å. Fredriksen, L. N. Mishra, and H. S. Byhring, *Plasma Sources Sci. Technol.* **19**, 034009 (2010).
- ²⁰P. C. Stangeby and J. E. Allen, *J. Plasma Phys.* **6**, 19 (1971).
- ²¹I. H. Hutchinson, *Plasma Phys. Controlled Fusion* **45**, 1477 (2003).
- ²²W. J. Miloch, J. Trulsen, and H. L. Pécseli, *Phys. Rev. E* **77**, 056408 (2008).
- ²³C. Charles, R. W. Boswell, and R. K. Porteous, *J. Vac. Sci. Technol. A* **10**, 398 (1992).
- ²⁴D. Gahan, B. Dolinaj, and M. B. Hopkins, *Rev. Sci. Instrum.* **79**, 033502 (2008).
- ²⁵T. Lafleur, C. Charles, and R. W. Boswell, *Phys. Plasmas* **16**, 044510 (2009).
- ²⁶H. S. Byhring, C. Charles, Å. Fredriksen, and R. W. Boswell, *Phys. Plasmas* **15**, 102113 (2008).
- ²⁷L. Patacchini and I. H. Hutchinson, *Plasma Phys. Controlled Fusion* **52**, 035005 (2010).